

Comparison of Reynolds Stress Estimates Derived from Standard and Fast-Ping ADCPs

NICHOLAS J. NIDZIEKO, DEREK A. FONG, AND JAMES L. HENCH

Environmental Fluid Mechanics Laboratory, Stanford University, Stanford, California

(Manuscript received 27 June 2005, in final form 14 November 2005)

ABSTRACT

A field experiment was conducted to directly compare the effects of different sampling modes on Reynolds stress estimates calculated from acoustic Doppler current profilers (ADCPs). Two 1.2-MHz ADCPs were deployed concurrently over a fortnightly cycle: one collected single-ping measurements using mode 1 and a second ADCP employed the fast-ping rate mode 12 with subping-averaged data recorded at the same sample rate as the first ADCP. While mode 12 clearly has a lower noise floor for the estimate of mean velocities, it has been an open question whether the averaging of subpings leads to a biased estimate of turbulence quantities, due to the temporal averaging inherent in this approach. Using the variance method, Reynolds stresses were estimated from the two ADCP datasets and compared with stresses computed directly from the velocity records obtained with a pair of fast sampling acoustic Doppler velocimeters (ADV) collocated with the ADCPs. Mode-12 stresses were more accurate than mode 1 in comparison to ADV-derived stresses, and mode 12 exhibited much lower measurement uncertainty than mode 1. Mode 1 appears to overestimate stresses by 20% in this study. The lower noise floor associated with mode 12 suggests that the variance method may be used with mode 12 to resolve smaller stresses than would be possible with mode 1.

1. Introduction

The acoustic Doppler current profiler's (ADCP's) ability to measure profiles of mean current and turbulent stresses, and hence turbulent shear production throughout the water column, has made it an invaluable tool in studies of vertically sheared flows where bottom or surface boundary layers compose a significant portion of the water column. The increasing popularity of the ADCP is at least partially due to its non-intrusive measurement method, its tolerance to biofouling, and its ability to synoptically sample nearly the entire water column. These capabilities are particularly well suited for work in shallow systems where ADCPs have been used to observe currents and dynamical quantities such as Reynolds stresses (Stacey et al. 1999b), near-bed velocity gradients (Fugate and Chant 2005), eddy viscosity (Rippeth et al. 2002), and tidal straining mechanisms (Simpson et al. 2005).

In highly frictional systems, the behavior of turbulent Reynolds stresses (e.g., Kundu and Cohen 2002) is often of interest and can be obtained from ADCP measurements using the difference of velocity variances between opposing beams (Lohrmann et al. 1990). Error analyses of the variance method (Stacey et al. 1999a; Lu and Lueck 1999; Williams and Simpson 2004) have demonstrated that uncertainties in Reynolds stress calculations are a combination of instrument- and flow-dependent noise and are inversely dependent on the number of samples, M , used in obtaining the variance estimate. Until recently, the ability to reduce error (by increasing M) was limited by the sampling rate of the ADCP (commonly 2 Hz), which is set by acoustical constraints and signal processing rates of the instrument hardware. Thus, ADCP measurements of large Reynolds stresses have been typically noisy and measurement of small Reynolds stresses problematic.

Ideally, one would have an instrument that could sample and record velocities at rates fast enough for resolution of turbulent fluctuations; however, this would require changes to the signal processing hardware found in the current generation of ADCPs. To partially address this issue, RD Instruments (RDI) re-

Corresponding author address: Nicholas J. Nidziko, Environmental Fluid Mechanics Laboratory, Stanford University, 380 Panama Mall, Terman M-13, Stanford, CA 94305-4020.
E-mail: nidziko@stanford.edu

cently introduced a firmware option that provides a faster-ping capability for their existing broadband ADCPs. This firmware option (known as water mode 12) allows an order of magnitude faster sampling rates (up to 20 Hz) by collecting a user-specified number of *unprocessed* subpings and then averaging the subpings into a single recorded velocity profile.

While mode 12 should produce velocity measurements with a lower uncertainty than could be obtained using standard ADCP signal processing (known as water mode 1), it is unclear whether an average of subpings will yield accurate estimates of turbulent Reynolds stresses. There is some suggestion that, while subping averaging reduces measurement uncertainty, significant turbulent fluctuations may be averaged out in the process. For example, Rippeth et al. (2002) showed that ensemble averaging single pings from standard mode-1 velocity profiles led to underestimated Reynolds stress magnitudes. Comparing different sampling rates and bin sizes, multiplying averaging resulted in a 23% underprediction of stress relative to the original signal. However, their study did not explore the higher sampling rates achievable with mode 12. The Williams and Simpson (2004, hereafter WS04), analysis of uncertainty in ADCP Reynolds stresses indicated that the reduction of instrument noise levels reduced stress estimate uncertainty by approximately a factor of 3 when using mode 12. A preliminary comparison was made to mode-1 data, but was somewhat inconclusive because their mode-12 and -1 data were collected at different times and locations.

A later study by Simpson et al. (2005) compared stress estimates derived from an acoustic Doppler velocimeter (ADV) to those from a mode-12 ADCP. The ADCP stresses were roughly 20% less than those from the ADV, but these differences may be attributable to the ADV not being collocated with the ADCP. Finally, recent work in coastal shelf regions (Howarth and Souza 2005; Souza and Howarth 2005) showed good agreement between collocated ADV and mode-12 ADCP stress estimates, at least during nonwavy conditions.

These previous studies have clearly demonstrated the utility of ADCPs for measuring Reynolds stresses. However, from an operational and technology standpoint, several questions remain. First, how do modes 1 and 12 compare directly? This is an important issue to resolve because mode 12 can consume 3–4 times as much battery power as mode 1, and thus may unnecessarily limit deployment durations. Second, if mode-1 and -12 Reynolds stresses differ, can we use an independent measure to determine which is correct? Third, do ADCP Reynolds stress estimates degrade with in-

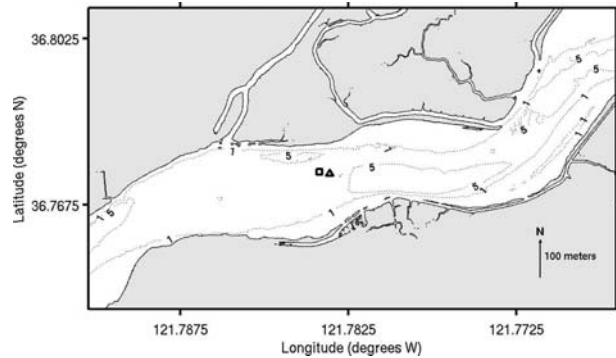


FIG. 1. Map of field experiment location within the main channel of Elkhorn Slough. Ocean is located 1 km west of moorings. Depth contours are in m below mean lower low water (MLLW). The locations of the mode 1 (\square) and mode 12 (\triangle) instruments are approximately 25 m apart. Gray shading indicates land above 0.75-m elevation.

creasing distance from the transducer (i.e., as the beams spread farther apart and the effective sample volume increases, is the estimate from bin 2 as accurate as bin 1)?

To address these questions we conducted an experiment to systematically compare the performance of the new fast-ping mode 12 with the standard mode 1 at the same site over a fortnightly period. The ADCP measurements are compared with simultaneously collected point velocity measurements from fast-sampling ADVs collocated with each ADCP.

2. Experimental setup

Two ADCP–ADV instrument frames were deployed in the main channel of Elkhorn Slough, California, during 12–28 October 2004 (Fig. 1). Elkhorn Slough is a shallow, tidal-forced system with a maximum tidal range of ~ 2.4 m, generating peak mean near-bed velocities of 0.7 and 0.4 m s^{-1} on ebb and flood, respectively, at the measurement site. In addition, the site was not affected by any significant surface waves that could have biased the measurement. We oriented the frames along the principal flow axis in a straight reach of the main channel in 6 m of water. The frames were placed approximately 25 m apart so that the ADCPs would not acoustically interfere with each other, yet close enough that the sampled flow properties would be similar.

Mounted on each frame was an RDI 1.2-MHz Workhorse Monitor ADCP and a Nortek 6-MHz Vector ADV. The westward ADCP was deployed in mode 1, sampling and recording at 1 Hz, and the eastward ADCP was deployed in mode 12, sampling 16 subpings at 40 m s^{-1} intervals for an effective data recording rate of 1 Hz (the 16 subpings are obtained in 0.64 s; while

processing and data logging increase the stored data rate to 1 s). Both ADCPs were configured with 0.25-m bins. To minimize errors due to instrument tilt (see Lu and Lueck 1999), the ADCPs were leveled to within 2° by divers during the deployment. Next to each ADCP, an ADV was mounted vertically, with the probe oriented upward, such that the sampling volume was coincident with the center of the ADCP bin located at 1 m above the bottom. The two ADVs were deployed with identical settings, sampling at 16 Hz and bursting for 600 s every half hour. An additional ADV was mounted on a third frame placed between the two ADCP-ADV frames, and set to measure at 1.25 m above the bottom coinciding with the second bin of the mode-12 ADCP.

3. Data analysis

Reynolds stresses were computed from the ADCP data using the variance method, as detailed in Stacey et al. (1999a, hereafter SMB). Along-beam velocities (b_i) were split into mean ($\overline{b_i}$) and fluctuating (b'_i) parts, where $I = 1:4$ represents the ADCP beam number. A 10-min averaging interval was chosen to obtain a statistically stationary turbulence field. The difference of the variance of opposing beams yields a Reynolds stress component, for example,

$$-\overline{u'w'} = \frac{\overline{b_2^2} - \overline{b_1^2}}{4 \sin\theta \cos\theta}, \quad (1)$$

$$-\overline{v'w'} = \frac{\overline{b_4^2} - \overline{b_3^2}}{4 \sin\theta \cos\theta}, \quad (2)$$

where u' , v' , and w' , are the respective along-channel, across-channel, and vertical velocity fluctuations; θ is the angle of the ADCP beam relative to vertical; and overbars represent the time averages. Principal component analyses on the ADCP and ADV velocities found that both instrument sites had very similar flow orientations (data not shown), and thus we used the same rotation on each to obtain along- and across-channel components.

Uncertainties in Reynolds stress estimates can be quantified following the error analysis described by SMB. The standard deviation of the Reynolds stress is a combination of instrument- and flow-dependent noise with the instrument noise defining a lower bound on the certainty of any given stress estimate. By averaging multiple subpings together, the uncertainty of the recorded velocity measurement is reduced thus lowering the mode-12 noise floor relative to mode 1.

For comparison to the ADCP estimates, ADV-derived Reynolds stresses were calculated directly from

raw earth coordinate velocities using a 10-min-averaging window. Diver observations indicated that in some instances large amounts of leafy green algae (*Ulva sp.*) obscured the ADV transducers, usually during strong ebb currents. Therefore, ADV samples with a beam correlation less than 0.85 were discarded, as were samples with along-channel velocity fluctuations exceeding 0.35 m s^{-1} . Bursts with more than 600 (out of 9600) discarded samples were not used for further analyses.

4. Results

Mean currents and estimated stresses from the mode-1 and -12 ADCPs are shown in Fig. 2. For presentation clarity, data from only one representative spring and neap cycle are shown. The along-channel component of velocity is tidally forced and exhibits semidiurnal variability (Figs. 2a,e), while the across-channel velocities are much weaker (Figs. 2b,f), showing some suggestion of secondary circulation. The peak currents and stresses appear to be larger at the western (mode 1) site and, as shall be discussed below, these differences appear to be due to spatial inhomogeneity in the flow field. Along-channel Reynolds stresses ($-\overline{u'w'}$; Figs. 2c,g) were strongest during ebb tides, and typically 2–4 times larger than across-channel Reynolds stresses ($-\overline{v'w'}$; Figs. 2d,h). The structure of the mean velocities was comparable for modes 1 and 12; however, Reynolds stress estimates from mode 1 were significantly noisier than from mode 12. This difference was particularly evident in the across-channel stresses, which were only discernable from noise for the mode-12 data. As such, we have omitted across-channel stress comparisons from further discussion.

As an independent check on the ADCP velocity and Reynolds stress values we compared them with ADV data (Fig. 3). For clarity, we compare the same representative tidal cycles as in Fig. 2. Mean velocities from both ADCPs (at bins centered 1 m above the bottom) were practically indistinguishable from the ADV values (Figs. 3a,c). The mode-1 stress estimates were noisy; nevertheless, they compare favorably to the ADV measurements with the exception of maximum spring ebb flows, when mode 1 overestimated the stress relative to the ADV. During this same period, the mode-12 stresses matched those of the ADV and exhibited considerably less noise than mode 1 (Figs. 3b,d).

Scatterplots of the along-channel stress derived from each ADCP-ADV pair are shown in Fig. 4. A linear least squares fit shows that mode 1 in general overestimates stresses in comparison to the ADV (Fig. 4a:

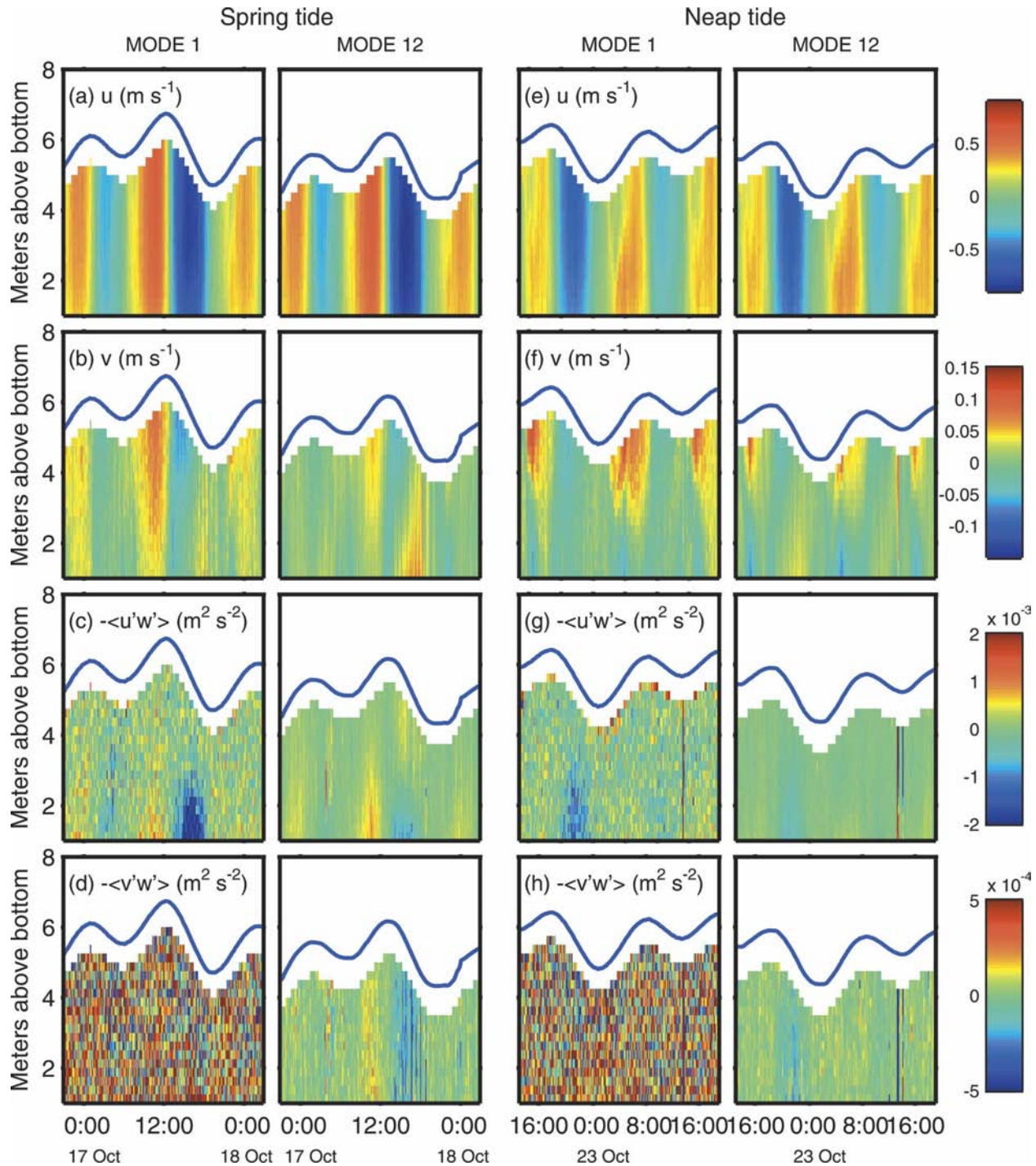


FIG. 2. (a), (e) Along-channel; (b), (f) cross-channel velocities; and (c), (d), (g), (h) Reynolds stresses for representative spring and neap tidal cycles for mode-1 and -12 ADCP data. Blue line represents water surface.

slope = 1.20 ± 0.09 , $r^2 = 0.66$), likely skewed by the overestimation of stress during spring ebb flows. The mode-12 and ADV stresses compare more favorably; within statistical uncertainty, there is a one-to-one correspondence between mode-12 and ADV stress esti-

mates (Fig. 4b: slope = 1.01 ± 0.04 , $r^2 = 0.86$). Comparison with a second ADV farther up in the water column (coinciding with ADCP bin 2) shows a similar level of agreement with mode 12 (data not shown: slope = 0.99 ± 0.05 , $r^2 = 0.75$) and there appears to be little

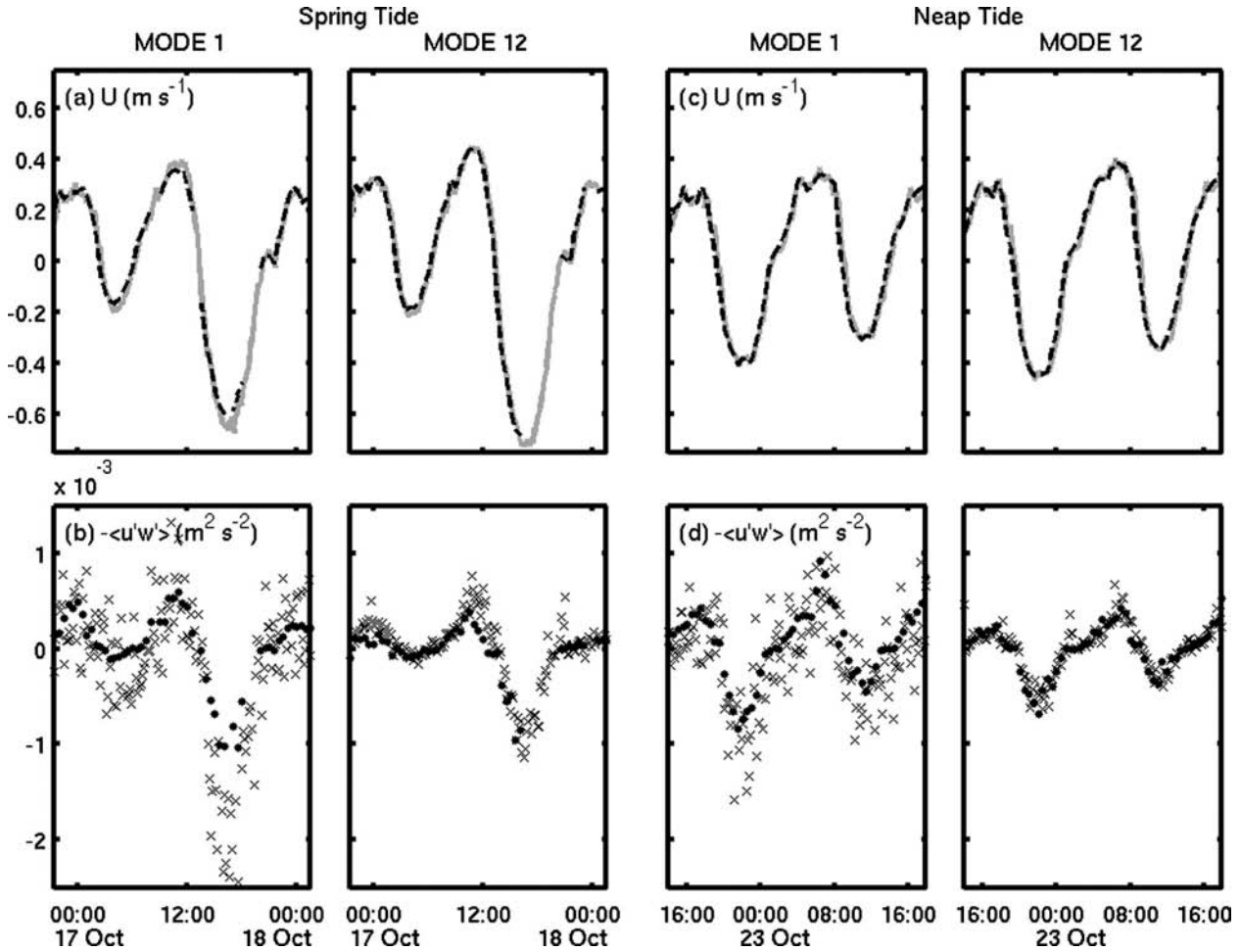


FIG. 3. (a), (c) Along-channel velocity and (b), (d) Reynolds stress comparison of ADCP (gray: solid, \times) and ADV (black: dashed, \bullet) data for same tidal cycles shown in Fig. 2. The center of ADCP bins and ADV sampling volume were both 1 m above the bottom. (a), (b) Data gaps in the spring tide ADV data are due to sensor obstruction from suspended vegetation.

degradation of Reynolds stress estimates between bins 1 and 2.

Noise level differences between modes 1 and 12 were evaluated following SMB and WS04, whereby the y intercept of the calculated Reynolds stress standard deviation plotted against the along-channel stress is proportional to the instrument noise. Using a least squares fit, and calculating a standard deviation from SMB [their Eqs. (26) and (28)], mode 1 had a minimum uncertainty of $1.84 \times 10^{-4} \text{ m}^2 \text{ s}^{-2}$ compared to $1.41 \times 10^{-5} \text{ m}^2 \text{ s}^{-2}$ for mode 12 (Fig. 5). This appreciable difference in Reynolds stress noise floor (a factor of 13 reduction) is consistent with the uncertainty expected from the square of the instrument noise level reduction between modes 1 and 12 [WS04, their Eq. (14)],

$$\sigma_R^2 = \frac{\sigma_N^4}{M \sin^2 2\theta}, \quad (3)$$

where σ_N^2 is the variance of the along-beam velocity due to instrument noise. Thus, the instrument noise level is reduced from $5.4 \times 10^{-2} \text{ m s}^{-1}$ to $1.5 \times 10^{-2} \text{ m s}^{-1}$ (mode 1 to 12, respectively), a factor of 3.6.

Representative power spectra of along-channel velocities for maximum ebb tide are shown in Fig. 6a for modes 1 and 12 and for one ADV (the spectrum for the other ADV is indistinguishable from the one shown). The spectrum for the ADV extends to 8 Hz, in comparison with 0.5 Hz for the ADCPs, by virtue of its higher Nyquist frequency. The ADV spectrum is the smoothest of the three, exhibiting an easily delineated spectral decay that closely follows the $-5/3$ slope expected for a turbulent inertial subrange. An inertial subrange is not readily seen in either ADCP spectra; however, mode 12 is in closer agreement to the $-5/3$ law than mode 1. The mode-1 power spectrum mimics the ADV spectrum only at the lowest frequencies. At

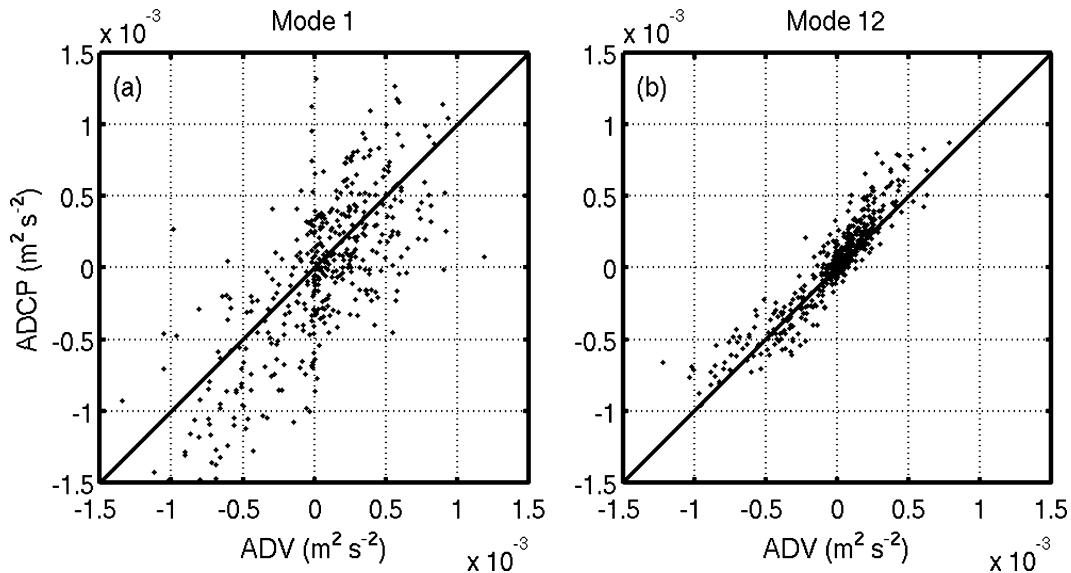


FIG. 4. Scatterplot of along-channel Reynolds stresses from collocated ADV and ADCP for the duration of the experiment. The solid line through each plot represents a 1:1 ratio: (a) mode 1, slope = 1.20 ± 0.09 , $r^2 = 0.66$ and (b) mode 12, slope = 1.01 ± 0.04 , $r^2 = 0.86$.

frequencies higher than ~ 0.1 Hz, the power rolls off slightly and it becomes impossible to differentiate the signal from white noise. In contrast, the mode-12 spectrum compares more favorably with the ADV spectrum

for a greater range of frequencies. It also flattens at higher frequencies, but still decays near the Nyquist frequency (0.5 Hz), suggesting a much lower noise floor than mode 1. Nevertheless, the agreement between the measured stresses (see Figs. 3 and 4) demonstrates that the mode-12 averaging of higher frequencies does not adversely effect the Reynolds stress estimates, at least in this field setting.

The time scale of the largest energy-containing eddies can be determined from the cross spectra of u' and w' , which we have plotted for a representative maximum ebb tide using data from one ADV, for clarity (Fig. 6b). In addition to the full 16-Hz data acquired from this ADV, we have plotted two additional datasets that were produced by resampling the ADV data using the sampling schemes similar to the ADCP modes: one dataset was created by subsampling velocities at 1 Hz; the second dataset was created by averaging the first 10 (out of 16) samples per second into a 1-Hz record, similar to the subping process performed in mode 12. The 16-Hz ADV record clearly shows a peak in energy centered at 0.16 Hz. The magnitude of this peak decreases at slack tide and is smaller on the weaker flood tide (not shown). These results compare well with theoretical time scales ($\kappa z/u^* \sim 4$ s) suggested in the literature (e.g., Pope 2000). This peak is captured by both resampling schemes; however, the noise at the Nyquist frequency of the 1-Hz subsampled data is greater than the velocity signal. The temporally averaged ADV data appears to remove this noise, as its spectrum closely resembles the original 16-Hz dataset.

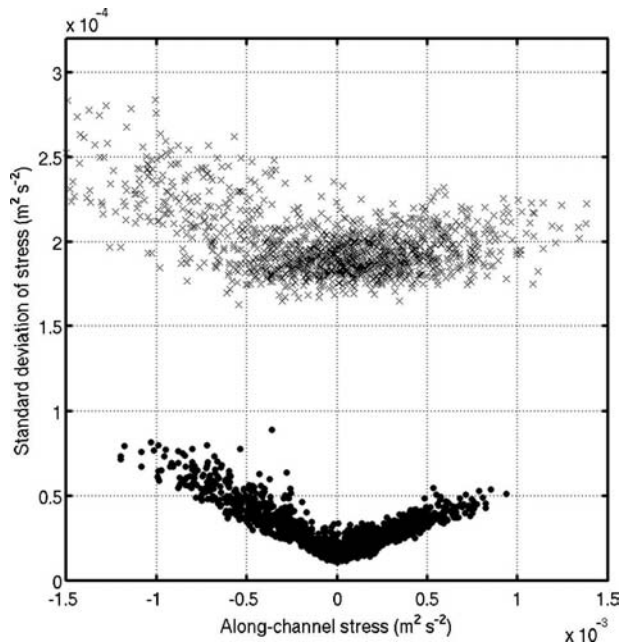


FIG. 5. The standard deviation of along-channel Reynolds stresses calculated from mode 1 (\times) and mode 12 (\bullet) ADCPs, plotted as a function of mean stress. The standard deviations were calculated following SMB, their Eqs. (26) and (28), $\sigma_R = \sqrt{(1/8M \sin^2\theta \cos^2\theta)\text{Var}(x_i'^2)}$, where $\text{Var}(x_i'^2)$ is the variance of along-beam velocity measurements.

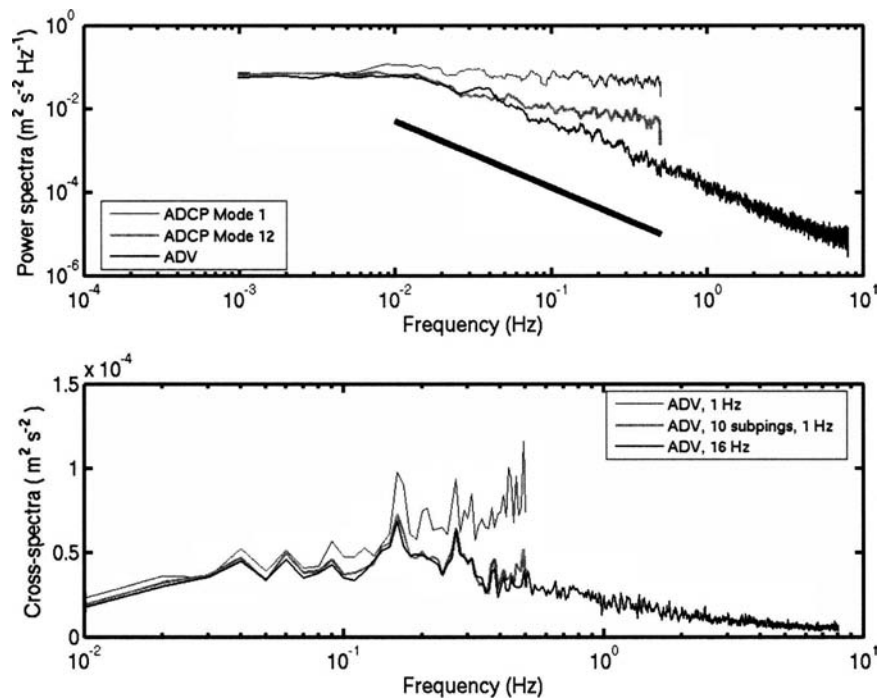


FIG. 6. (a) Power spectra of along-channel velocity fluctuations (u') from mode-1 and -12 ADCPs and one ADV. Spectra are ensemble averages of four bursts bracketing the maximum ebb tide. Solid black line represents $-5/3$ slope expected for an inertial subrange. (b) Cross spectra of along-channel (u') and vertical (w') velocity fluctuations from ADV shown in Fig. 6a. Raw 16-Hz data was subsampled at 1 Hz or burst averaged into 1-Hz data to represent ADCP sampling schemes. Cross spectra are presented in variance-preserving form.

This independent check supports the result that, in this field setting, the temporal averaging performed in mode 12 does not underestimate Reynolds stresses because the improvement in measurement accuracy far outweighs the loss of the limited energy contained in the higher frequencies. In addition, it appears that a portion of the Reynolds stress estimate from the mode-1 ADCP may be the result of a bias due to noise.

5. Discussion and conclusions

In this experiment, mode 12 produced more accurate Reynolds stress estimates and lower measurement uncertainty than mode 1 when compared to collocated ADVs. The temporal averaging performed in mode 12 produces a more accurate velocity measurement and thus allows better resolution of small stresses (e.g., low energy flows or secondary circulation in high energy environments) that would be indistinguishable from instrument noise if measured using mode 1. This temporal averaging of raw subpings did not result in an underestimate of stresses; however, it is quite possible that for some sites the turbulence climate might be such that significant energy is contained at frequencies higher

than 1 Hz. In these situations, mode-12-averaged subpings may result in an underestimate of the actual Reynolds stress. Mode 1, however, appears to *overpredict* Reynolds stresses by $\sim 20\%$ in our case, particularly in energetic flows. It appears that measurement noise biases the stress estimate, but this merits further study. It does suggest one possible contribution toward the imbalance in the turbulent kinetic energy (TKE) budget, such as in Rippeth et al. (2003).

There are two considerations for producing accurate ADCP estimates of Reynolds stress: the velocity signal must be fully resolved and the signal-to-noise ratio must be large enough to discern stress estimates from the background noise. The shortest temporal resolution is set by the Nyquist frequency of the sample rate; however, a practical limit to spectral resolution of a signal around the Nyquist frequency is ~ 2.5 times the frequency of interest (Emery and Thomson 1997). Thus, for a 1-Hz sampling scheme, turbulence frequencies up to 0.2 Hz should be readily resolvable, provided that the length scale can be resolved for the specified bin size. Furthermore, Reynolds stress estimates should be statistically different from zero, based upon the error of the measurement. Temporal averaging has the poten-

tial to improve signal-to-noise ratio markedly; however, caution should be exercised such that any averaging scheme used does not filter out significant energy from the velocity measurements. The subping process in mode 12 allows the averaging interval to be condensed into the first (in our case) 0.64 s, effectively removing frequencies higher than ~ 1.5 Hz, without averaging out any of the more significant energy-containing scales. In light of this and the findings of the present study, until the technology emerges that allows every fast ping to be stored as data, we suggest mode 12 should be considered in situations where resolution of small stresses is desired.

Acknowledgments. We thank J. Douglas, J. Felton, and S. Hansen from Moss Landing Marine Laboratories, as well as K. Davis, J. Nomura Fong, J. Rosman, and A. Santoro from Stanford University for assistance in the field deployment. Comments by A. Boehm, S. Monismith, J. Simpson, A. Souza, and M. Stacey were particularly helpful in the preparation of the manuscript. Comments of two anonymous reviewers were appreciated in the final revision of the manuscript. We also gratefully acknowledge support from NSF (ECS-0308070) and the California Bay-Delta Authority (ERP-02D-P51, 46000001955).

REFERENCES

- Emery, W. J., and R. E. Thomson, 1997: *Data Analysis Methods in Physical Oceanography*. Pergamon, 634 pp.
- Fugate, D. C., and R. J. Chant, 2005: Near-bottom shear stresses in a small, highly stratified estuary. *J. Geophys. Res.*, **110**, C03022, doi:10.1029/2004JC002563.
- Howarth, M. J., and A. J. Souza, 2005: Reynolds stress observations in continental shelf seas. *Deep-Sea Res.*, **52**, 1075–1086.
- Kundu, P. J., and I. M. Cohen, 2002: *Fluid Mechanics*. Academic Press, 730 pp.
- Lohrmann, A., B. Hackett, and L. D. Roed, 1990: High resolution measurements of turbulence, velocity, and stress using a pulse-to-pulse coherent sonar. *J. Atmos. Oceanic Technol.*, **7**, 19–37.
- Lu, Y., and R. G. Lueck, 1999: Using a broadband ADCP in a tidal channel. Part II: Turbulence. *J. Atmos. Oceanic Technol.*, **16**, 1568–1579.
- Pope, S. B., 2000: *Turbulent Flows*. Cambridge University Press, 771 pp.
- Rippeth, T. P., E. Williams, and J. H. Simpson, 2002: Reynolds stress and turbulent energy production in a tidal channel. *J. Phys. Oceanogr.*, **32**, 1242–1251.
- , J. H. Simpson, and E. Williams, 2003: Measurement of the rates of production and dissipation of turbulent kinetic energy in an energetic tidal flow: Red Wharf Bay revisited. *J. Phys. Oceanogr.*, **33**, 1889–1901.
- Simpson, J. H., E. Williams, L. H. Brasseur, and J. M. Brubaker, 2005: The impact of tidal straining on the cycle of turbulence in a partially stratified estuary. *Cont. Shelf Res.*, **25**, 51–64.
- Souza, A. J., and M. J. Howarth, 2005: Estimates of Reynolds stress in a highly energetic shelf sea. *Ocean Dyn.*, **55**, 490–498.
- Stacey, M. T., S. G. Monismith, and J. R. Burau, 1999a: Measurements of Reynolds stress profiles in unstratified tidal flow. *J. Geophys. Res.*, **104**, 10 933–10 949.
- , —, and —, 1999b: Observations of turbulence in a partially stratified estuary. *J. Phys. Oceanogr.*, **29**, 1950–1970.
- Williams, E., and J. H. Simpson, 2004: Uncertainties in estimates of Reynolds stress and TKE production rate using the ADCP variance method. *J. Atmos. Oceanic Technol.*, **21**, 347–357.

Copyright of *Journal of Atmospheric & Oceanic Technology* is the property of *American Meteorological Society* and its content may not be copied or emailed to multiple sites or posted to a listserv without the copyright holder's express written permission. However, users may print, download, or email articles for individual use.